Scientia Iranica, Vol. 10, No. 3, pp 287-299

SCIENTIA
IRANICA

Prediction of Furnace Run Length for the Pyrolysis of Naphtha by a PC Based Simulator

A. Niaei[1], J. Towfighi* and M. Sadrameli[1]

The reaction mechanism of the thermal cracking of hydrocarbons is generally accepted as a free-radical chain reaction. Using a rigorous kinetic model, a complete reaction network for the decomposition of the naphtha feed has been developed by the Process Engineering Group of Tarbiat Modarres University and is used for the simulation of a naphtha cracker. For studying the pyrolysis reaction kinetics, a computer control pilot plant system has been designed and assembled. Experiments on the thermal cracking of naphtha were carried out in a tubular reactor under conditions as close as possible to those in industry. Taking into account the kinetics of coke formation, along with the simultaneous simulation of the reactor and firebox, provides a detailed understanding and an accurate prediction of the industrial cracking furnace behavior and run length.

INTRODUCTION

Pyrolysis of naphtha is an important commercial process for the production of ethylene, propylene and 1,3-butadiene. The reactions are always accompanied with the formation of coke, which deposits on the walls of the tubular reactors. Under typical operating conditions, coke formation from naphtha pyrolysis is about 0.01 wt% of the feed. The formation and deposition of coke on the inner surface of the coils has major consequences for operation of the furnace. Firstly, the coke layer reduces heat transfer from the furnace to the process gas. If feed conversion is to be maintained, a higher heat input to the furnace is required, resulting in a rise in the external tube skin temperature and a decrease in the thermal efficiency of the furnace. The tube skin temperature gradually increases over a period of time and approaches a maximum value, which is imposed by the tube metallurgy. The operation has to be stopped to decoke the reactor tubes by controlled combustion of the coke layer with a steam/air mixture. Secondly, coke deposition on the internal tube skin reduces the cross section of the reactor tube. With a constant feed rate to the reactor coil, the pressure drop over the reactor tube increases. Since the process gas outlet pressure is normally imposed, the feed inlet pressure increases during the run length and this is detrimental to the ethylene selectivity. Increasing the inlet pressure can also cause the cracking run to be stopped for decoking the tubes. Reactor geometry, operating conditions and feed stock composition determine which of the two described effects dominates the production cycle to be stopped. Since decoking means a loss in production capacity, there is a strong need for assessing coke formation from a variety of feedstocks and for predicting the run time of a furnace.

The aim of this study is to investigate the accuracy of a rigorous kinetic model for the pyrolysis of naphtha and to reach an agreement between the calculated results and experimental data. This paper also describes the use of certain simulation software, which was developed in the Process Engineering Group of Tarbiat Modarres University [1], for the prediction of radical reactions, coke formation and firebox calculations in industrial naphtha cracking furnaces.

EXPERIMENTAL SECTION

Pyrolysis experiments were conducted in a tubular pilot plant system, which was designed and assembled by the Process Engineering Group for studying pyrolysis

1. *Department of Chemical Engineering, Tarbiat Modarres University, P.O. Box 14155-4838, Tehran, I.R. Iran.*
*. *Corresponding Author, Department of Chemical Engineering, Tarbiat Modarres University, P.O. Box 14155-4838, Tehran, I.R. Iran.*

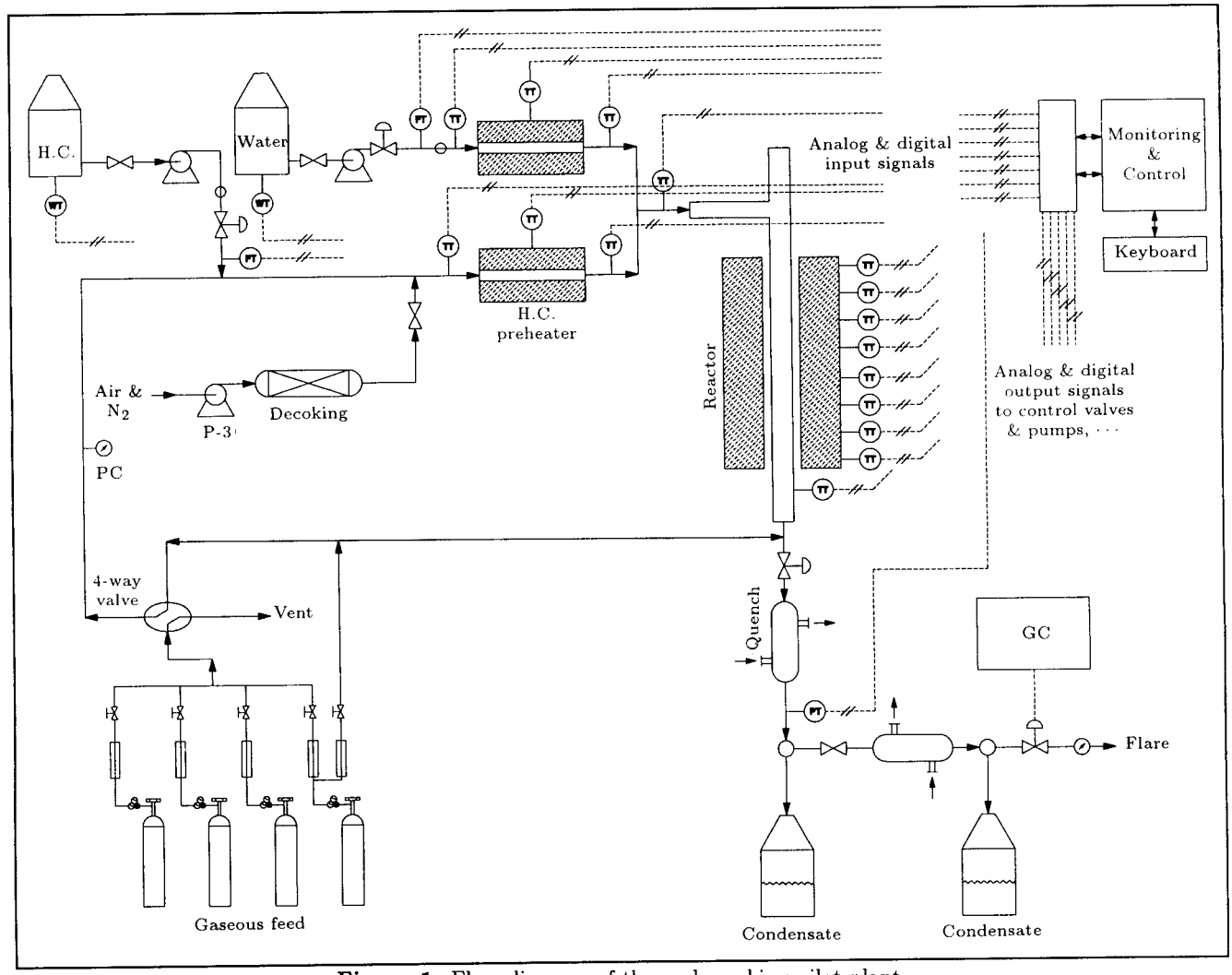

Figure 1. Flow diagram of thermal cracking pilot plant.

reaction kinetics. The setup, shown schematically in Figure 1, is a computer controlled pilot plant unit, used for experiments in naphtha thermal cracking. The unit consists of the following three main sections.

Operating Section

The operating section includes the feeding, preheating, reaction and quench parts. Both gaseous and liquid hydrocarbons can be fed. The hydrocarbon and diluent water are pumped into the preheaters and gas flow is metered by means of mass flow controllers. Liquid hydrocarbons and water, as dilution steam, are fed by means of dowsing and pulsation-free pumps. The vessels containing the liquid feedstock are placed on digital balances, which are connected to the on-line computer for feed monitoring. The setpoint of the pumps are set manually. The hydrocarbon and steam are preheated to 600°C and mixed.

The furnace consists of two electrical preheaters for the water and hydrocarbon feeds and an additional electrical heater is used for the reactor section. The preheaters are single zones and the reaction section heater is divided into eight zones, which can be heated independently to set any type of temperature profile. Each zone power can be controlled manually or by a control algorithm implemented into the process computer. The reactor is a 1000 mm long, 10 mm internal diameter tube, made of Inconel 600. There are eighteen thermocouples along the reactor, 8 inside the furnace, 8 on the external tube skin and an additional 2 for the measuring of XOT (Cross Over Temperature) and COT (Coil Outlet Temperature). The reactor is heated electrically and placed vertically in a cylindrical furnace. The analog signals of the thermocouples are connected to the process computer and the temperature reading is also visualized on a color digital thermometer display.

The reactor effluent is cooled in a double pipe heat exchanger by circulating ice water. Liquid products, tars and any possible solid particles are cooled and

separated by means of three glass condensers and cyclones. The cyclone is followed by a condenser, in which steam and heavy products are condensed and kept in a circulating ice water bath to maintain a constant temperature. A fraction of product gas is then withdrawn for on-line analysis using gas chromatographs, while the rest is sent directly to the flare.

Analysis Section

The on-line analysis of the reactor effluent is performed by means of two computerized gas chromatographs. First a Varian Chrompack CP3800, with a two Flame Ionization Detector (FID), analyses the light components, including hydrogen, methane, oxygen, carbon monoxide, carbon dioxide, light hydrocarbons up to C_4 and internal standard nitrogen. The second Varian Chrompack CP3800 has two detectors, a Thermal Conductivity Detector (TCD), which analyses the light components, including hydrogen, and one Flame Ionization Detector (FID), for the analysis of heavy components (PIONA), including C_{5+} and aromatics. The analysis of the GC systems was carried out under the conditions given in Table 1.

Control Section

The PIII process computer is connected on-line to the pilot plant and controls the main part of the unit. The connection with the pilot plant is maintained through Analog to Digital (A/D) converters, Digital to Analog (D/A) converters and digital input-outputs. The on-line computer control software developed by the research group, can be divided into two main parts of monitoring and control. In the monitoring section, the process gas, tubeskin and heaters wall temperatures are displayed on a screen by means of a visual C program in a 32-bit Windows Operating System. Water and hydrocarbon flow rates are calculated from the weight change on the digital balances and the sampling rate. Monitoring of digital balances is achieved by means of a visual basic program, which was developed by the AND company. In the control section, the temperature profile of the reactor is stabilized by the temperature controlling of each zone, by means of a conventional PID controller. The set points for this temperature stabilizing control are included in the software. All pilot plant measurements and control systems information are saved in the text and graphical mode.

The experiments were conducted at atmospheric pressure in the coil outlet temperature range of 800-870°C. The dilution steam ratio, H_2O/naphtha, was 0.6-0.8 and the residence time was varied from 0.2-0.5 sec. The preheating temperature range was 580-600°C. The feedstock was straight run naphtha from the Arak Petrochemical Corp., with the composition as used in the plant itself.

MODEL EQUATIONS AND SIMULATION PROCEDURE

Kinetic Model

The reaction mechanism of the thermal cracking of hydrocarbons is generally accepted as a free-radical chain reaction. A complete reaction network, for the decomposition of the naphtha feed was developed [1], using a rigorous kinetic model, and is used for the simulation of a naphtha cracker.

The dimensions and complexity of the detailed kinetic models of hydrocarbon pyrolysis imposes and justifies the adoption of a proper simplification level, coherent with the final aim of the model itself. These simplifications and/or lumping procedures reduce the total number of equivalent chemical species and equivalent reactions.

The very detailed mechanistic kinetic scheme in this simulation network, developed by Towfighi et al. [2-4] during the last decades, includes over a thou-

Table 1. Specification of analysis system.

Chromatograph			
1.Varian Chrompack CP3800			
		Detector	**Product Analysis**
Column A	Capillary CP-CIL 5CB	FID	$C_2H_4, C_3H_6, C_4H_6, \ldots$
Column B	Packed column	Methanizer and FID in series	CO, CO_2
2.Varian Chrompack CP3800			
Column A	Capillary CP - CIL-PONA	FID With split/splittless	C_{5+}, aromatics
Column B	Packed column	TCD	H_2, CH_4

sand reactions and 91 molecular and radical species. As usual, this chain radical mechanism consists of several radical and molecular elementary reactions, which can be briefly summarized as follows:

A. Radical reactions:

1. Initiation reactions:
   Unimolecular:

$$CH_3 - (CH_2)_4 - CH_3 \rightarrow$$

$$C_2H_5\bullet + CH_3 - CH_2 - CH_2 - CH_2\bullet$$

   Bimolecular:

$$CH_3 - CH_3 + CH_2 = CH_2 \rightarrow C_2H_5\bullet + C_2H_5\bullet$$

2. Propagation reactions:
   Radical decomposition is one of the most important reaction types and directly produces ethylene, according to the following scheme:

$$\bullet CH_2 - CH_2 - CH_3 \rightarrow C_2H_4 + CH_3\bullet$$

   Radical isomerization:

$$\bullet CH_2 - (CH_2)_3 - CH_2 - CH_3 \rightarrow$$

$$CH_3 - (CH_2)_3 - \dot{C}H - CH_3.$$

   H-abstraction on molecules:

$$CH_3\bullet + CH_3 - CH_2 - CH_3 \rightarrow$$

$$CH_4 + CH_3 - CH_2 - CH_2\bullet$$

   Addition of radicals on unsaturated molecules:

$$CH_3\bullet + CH_2 = CH - CH_3 \rightarrow$$

$$CH_3 - CH_2 - CH_2 - CH_2\bullet$$

3. Termination reactions:
   Recombination of radicals to form one molecule:

$$C_2H_5\bullet + C_2H_5\bullet \rightarrow CH_3 - CH_2 - CH_2 - CH_3.$$

   Recombination of radicals forming two molecules:

$$C_2H_5\bullet + C_2H_5\bullet \rightarrow CH_3 - CH_3 + CH_2 = CH_2.$$

B. Molecular reactions:
   Olefin isomerization:

$$CH_3 - CH = CH - CH_3 \rightarrow CH_2 = CH - CH_2 - CH_3.$$

   Olefin dehydrogenation:

$$CH_2 = CH - CH_2 - CH_3 \rightarrow$$

$$CH_2 = CH - CH = CH_2 + H_2.$$

   Olefin decomposition:

$$CH_2 = CH - CH_2 - CH_2 - CH_3 \rightarrow$$

$$CH_2 = CH - CH_3 + CH_2 = CH_2.$$

   Diels-Alder reaction:

$$CH_2 = CH - CH = CH_2 + CH_2 = CH_2 \rightarrow$$

$$\text{Cyclo } C_6H_{10}.$$

On the basis of these intrinsic kinetic parameters, it was possible to describe the primary pyrolysis reactions of all the different hydrocarbon species and the generation of these reaction mechanisms allowed the development of very large kinetic schemes. Due to these dimensions, the extensive use of grouping and lumping rules allows one to define a very effective flexible lumping procedure for naphtha feedstock.

The governing mass, energy and momentum balance equations for the cracking coil constitute the two-point boundary value problem, which has a significant stiffness in the numerical simulation due to the large differences in concentration gradient between radicals and molecules. This problem can be tackled through application of the Gear method. Details of the solution may be obtained from Towfighi et al. [2]. In Figures 2 to 4 the yields of various cracking products are plotted against the severity index. These results were obtained for the cracking of naphtha at different coil outlet temperatures. In general, with an increase in severity, the yield of propylene increases and attains a maximum value, while thermally stable methane, ethylene and aromatic yields will be slightly decreased. Methane and benzene are thermally quite stable. Aromatics are also formed by a reaction between the cracking products of olefins and diolefins. Toluene, on the other hand, undergoes dealkylation reactions and, thus, attains a maximum value. In the experimental process, the above mentioned trend

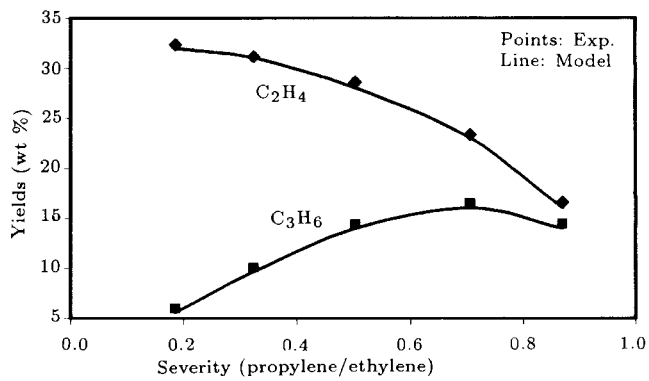

Figure 2. Variation of ethylene and propylene with severity.

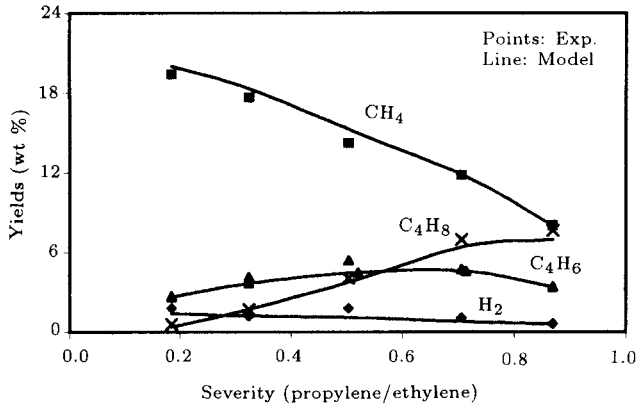

Figure 3. Variation of hydrogen, methane, butene and 1,3 butadiene with severity.

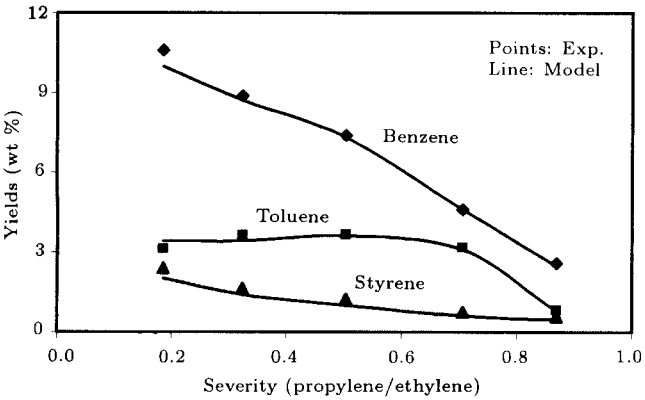

Figure 4. Variation of aromatic compounds with severity.

has been also observed. The calculated values from the kinetic reaction network (developed by the Process Engineering Group), for each product yield in naphtha pyrolysis, is in good agreement with the experimental data.

Reactor Model

A one dimensional plug flow model is used to simulate the thermal cracking reactor. The set of continuity equations for the various process gas species is solved, simultaneously, with the energy, momentum and coking rate equations required [5]. These equations are as follows:

Mass balance:

$$\frac{dF_j}{dz} = \Big(\sum_i S_{ij} r_{ri}\Big)\frac{\pi d_t^2}{4}. \tag{1}$$

Energy balance:

$$\sum_j F_j c_{pj} \frac{dT}{dz} \equiv Q(z)\pi d_t + \frac{\pi d_t^2}{4}\sum_i r_{ri}(-\Delta H)_i. \tag{2}$$

Momentum balance:

$$\Big(\frac{1}{M_m P_t} - \frac{P_t}{\eta . G^2 RT}\Big)\frac{dp_t}{dz} = \frac{d}{dz}\Big(\frac{1}{M_m}\Big) + \frac{1}{M_m}\Big(\frac{1}{T}\frac{dT}{dz} + Fr\Big). \tag{3}$$

With the friction factor:

$$Fr = 0.092\frac{\mathrm{Re}^{-0.2}}{d_t}. \tag{4}$$

For the straight parts of the reactor coils:

$$Fr = 0.092\frac{\mathrm{Re}^{-0.2}}{d_t} + \frac{\zeta}{\pi R_b}, \tag{5}$$

and for the tube bends:

$$\zeta = (0.7 + 0.35\frac{\Lambda}{90^\circ})(0.051 + 0.19\frac{d_t}{R_b}), \tag{6}$$

where R_b and Λ represent the radius of the tube bend and angle of bend, respectively.

Since the coking is slow, quasi steady state conditions may be assumed, so that the rate of coke formation [6] may be written as:

$$\frac{\partial C}{\partial t} = (d_t - 2t_c)\frac{\alpha . r_c}{4\rho_c}. \tag{7}$$

Using the mathematical model, the amount of coke deposited on the internal wall of the reactor tubes has been calculated with a limiting value for tube skin temperature (1050°C). In the following, the effect of the coke thickness on the operating parameters has been demonstrated in the on-stream time of the furnace.

Coking Model

Coke formation in the pyrolysis of hydrocarbons is a complex phenomena. Three mechanisms contribute to the deposition of a coke layer. First, catalytic coking occurs on the clean and bare tube with a high weight percent of Ni and Fe that catalyze dehydrogenation of hydrocarbons at elevated temperatures. It has been experimentally observed that the rate of coke deposition is, initially, high and gradually decreases to a constant asymptotic value as reaction proceeds. The high initial rates are due to the catalytic effects of the metal surface on the coke forming reactions and, as the coke layer builds up, the catalytic activity is progressively reduced. At this stage, the catalytic activity of the metal particle diminishes and both carbon formation and CO production slow down. This phenomena occurs some time after the regular start up of the cracking coils and similar trends for the

coking rate have been reported on all metal alloys in the pyrolysis of hydrocarbons [7]. The second and main mechanism is the asymptotic coking that occurs during the on stream-time of the cracking process. In this mechanism, interaction between active sites on the coke layer and the gas phase species takes place. The active sites are free radicals and originate from hydrogen abstraction by small active gas phase radicals, such as hydrogen and methyl radicals. At the free radical sites, unsaturated precursors from the gas phase react via addition, followed by a set of dehydrogenation and cyclization reactions, finally yielding a graphitic coke layer. A third mechanism involves the formation of droplets in the gas phase, which, then, impinge and adhere to the surface and are incorporated in the coke layer, especially in heavy liquid feedstocks [7].

In the present paper, a number of coke precursors were found to contribute to the formation of coke. Unsaturates and aromatics are a very important class of coke precursors. They are reaction products of the pyrolysis reactions so that their concentration in the high temperature zone of the reactor is high. Unsaturates are reactive and are good candidates for radical addition. Also, aromatic ring structure is close to the structure of the coke matrix. Further, (branched) aromatics are reactive components, especially at the high temperatures prevailing in thermal cracking coils. From literature survey and plant data, a coking model, in which a number of coke precursors and the relative rates of coke deposition contributed to the formation of coke [8-11]. The precursors are classified into different groups, such as olefinic (ethylene, propylene, 1-butene,...), acetylenic (acetylene, methyl acetylene, ethyl acetylene, vinyl acetylene), aromatics (benzene, toluene, xylene, styrene,...) and C_{5+} (unsaturated). The residual sum of squares between the calculated values and asymptotic coking rates (literature and plant observations) was used as the objective function and the coking kinetic parameters were estimated by using Marquardt algorithm. The following expression can, thus, be written for the rate of coke formation for contributed precursors:

$$r_c = k_{\text{olefins}} C_{\text{olefins}}^{n_1} + k_{\text{Actylenic}} C_{\text{Actylenic}}^{n_2} + k_{\text{Aromatics}} C_{\text{Aromatics}}^{n_3} + k_{C_{5+}} C_{C_{5+}}^{n_4}, \quad (8)$$

where:

$$k_i = k_0 . \exp(-E_0/RT). \quad (9)$$

The coke formation takes place at the temperature of the gas/coke interface and the kinetic parameters of coking are presented in Table 2.

Table 2. Kinetic parameters of coke formation.

Coke Precursors	k_0	E_0	n
Olefinic	3.412 E 11	241250	1.9
Acetylenic	8.14 E 12	200890	1.5
Aromatics	6.14 E 10	189560	1.4
C_{5+} (unsaturates)	3.412 E 14	212260	1.62

Furnace Model

The configuration of the reactor coil inside the furnace, consisting of a number of straight vertical tubes called passes connected by bends and the positioning and type of the burners, require special attention. With the help of an accurate simulation for the radiative heat exchange in a furnace, calculation of the temperature and heat flux distributions in the firebox and the reactor can be achieved. Simulation of the firebox was developed by Hottel and Sarofim [12], and Paramenswaran et al. [13]. The multi zone mathematical model has been used by Sadrameli [14] for simulation of the cracking furnaces, assuming a one dimensional conduction heat transfer in the tubes. In the present work, this model is extended to the three-dimensional model and has been applied to simulate the thermal cracking furnaces of the Arak Olefin Plant. The furnace refractory walls, surface reactor coils and flue gas volume were discretized into a number of isothermal surface and volume zones with uniform properties. For calculation of the direct and total-exchange areas, a fundamental approach, considering individual band absorption by carbon dioxide and water, is taken. In addition, the position of the burners in the furnace walls and the flue gas flow pattern in the firebox are explicitly accounted. Zone method involves subdivision of the radiating enclosure into isothermal volume and surface zones. Mathematical models based on the zone method vary in complexity, depending on the number and arrangement of zones. Three main types of zone model can be identified:

- Single-gas zone model; this model assumes uniform gas temperature and composition.
- Long-furnace model; this one dimensional model consists of a longitudinal series of well-stirred zones, where the enthalpy of the combustion products leaving one zone is the same as input.
- Multi-dimensional zone model: This model is used when both longitudinal and cross sectional or radial variation in temperature and heat flux are expected to be important. In this model, the furnace refractory walls, tubes and flue gas volume are divided into a number of isothermal surface and volume elements with uniform properties. The energy balance, containing contribution of radiative, convective and/or

conductive heat exchange, is constructed for each of these elements, resulting in a set of non-linear algebraic equations in the form:

$$\begin{bmatrix} \cdots & Z_1Z_1 - \sum Z_iZ_j & \cdots \\ \cdots & Z_1Z_2 & \cdots \\ \cdots & \cdots & \cdots \\ \cdots & \cdots & \cdots \\ \cdots & \cdots & \cdots \\ \cdots & Z_1Z_n & \cdots \end{bmatrix}$$

$$\begin{bmatrix} Z_2Z_1 & \cdots & Z_nZ_1 \\ Z_2Z_2 - \sum Z_2Z_2 & \cdots & Z_nZ_2 \\ \cdots & \cdots & \cdots \\ \cdots & \cdots & \cdots \\ \cdots & \cdots & \cdots \\ Z_2Z_n & \cdots & Z_nZ_n - \sum Z_nZ_j \end{bmatrix} \cdot$$

$$\begin{bmatrix} E_1 \\ E_2 \\ \cdots \\ \cdots \\ E_n \end{bmatrix} = \begin{bmatrix} Q_1A_1 \\ Q_2A_2 \\ \cdot \\ \\ Q_nA_n \end{bmatrix} . \tag{10}$$

The matrix element Z_iZ_j represents the total exchange area between the zones Z_i and Z_j. This is the amount of radiative energy emitted by zone Z_i and absorbed, both directly and after reflection on other zones, by zone Z_j and divided by the black body emissive power, E_i. The emissive of a black body with temperature T_i is given by the Stefan-Boltsmann law. Calculation of the total exchange area for flue gas volume, refractory wall zones and tube surface zones, was discussed in detail by Rao et al. [15]. The non-radiative heat flux emitted by zone Z_i is represented by Q_i.

Solving the set of energy balances yields the heat flux and temperature distribution in the furnace. When the reactor tubes are discretized in an axial direction only, heat flux profiles, $q(z)$, and external tube skin temperature profiles, $T_{\text{ext}}(z)$, are obtained. When the tubes are also discretized along the perimeter, heat flux profiles, $T(r,\theta,z)$, are obtained. The conduction equations for each axial tube zone with the appropriate boundary conditions are:

$$\frac{1}{r}\frac{\partial}{\partial r}\left[kr\frac{\partial T}{\partial r}\right] + \frac{1}{r^2}\frac{\partial}{\partial \theta}\left[k\frac{\partial T}{\partial \theta}\right] + \frac{\partial}{\partial z}\left[k\frac{\partial T}{\partial z}\right] = \rho C_p\frac{\partial T}{\partial t}. \tag{11}$$

By assuming that the temperature in each small element is constant, Equation 11 can be simplified as:

$$\nabla^2 T = \frac{\partial^2 T}{\partial r^2} + \frac{1}{r}\frac{\partial T}{\partial r} + \frac{1}{r^2}\frac{\partial^2 T}{\partial \theta^2} = 0. \tag{12}$$

The boundary conditions for Equation 12 are now defined in the internal and external surface of the coils as:

at $r = r_{\text{ext}}$:

$$k\frac{\partial T}{\partial r}(r,\theta) = q(r,\theta), \tag{13}$$

at $r = r_{\text{int}}$:

$$k\frac{\partial T}{\partial r}(r,\theta) = h_p[T(r,\theta) - T_p], \tag{14}$$

$$T(r,\theta) = T(r,\theta+\pi), \tag{15}$$

$$\frac{1}{r}\frac{\partial T(r,\theta)}{\partial \theta} = \frac{1}{r}\frac{\partial T(r,\theta+\pi)}{\partial \theta}. \tag{16}$$

The discretization of the above equations was discussed in detail by Heynderickx and Cornelis [16]. The calculation module for the circumferential temperature profiles is coupled to the furnace and reactor simulation model.

Simulation Procedure

A simplified flowchart of the iterative calculation scheme is given in Figure 5. Predicting the run length of the industrial cracking furnace requires the simultaneous solution of the rigorous kinetic model for the pyrolysis of naphtha. The coking model and the energy balance in the fire box formed Equations 1-3, 7, 10 and 12. To do so, the run time is increased in a stepwise manner. Incremental pseudo steady state is assumed for the coking, since the main cracking reactions are much faster than the coke formation. Starting from initial estimates for temperatures, fluxes and recycle gas composition, the energy balances (Equations 10 and 12) are solved and better estimates for the zone temperatures provided. New flux estimates are calculated from the tube skin and process gas temperatures. Based on these new fluxes, process and recycled gas composition, temperature and pressure are calculated from Equations 1 to 3. By solving Equation 12, new zone temperatures are obtained, which are compared to the previously obtained values. The cycle is repeated until convergence is reached for the time increment. For the present simulation, a run time increment of 50 h was found to be appreciative. For each time increment, a coupled furnace and reactor simulation is performed.

Tables 3 to 7 represent basic information about the industrial cracking furnace, the split coil reactors and the operating conditions and Figure 6 shows the configuration of coils. The furnace considered in this work contains eight split coils in a staggered row configuration; each making eight passes through the furnace. Because of symmetry, only two reactor coils had to

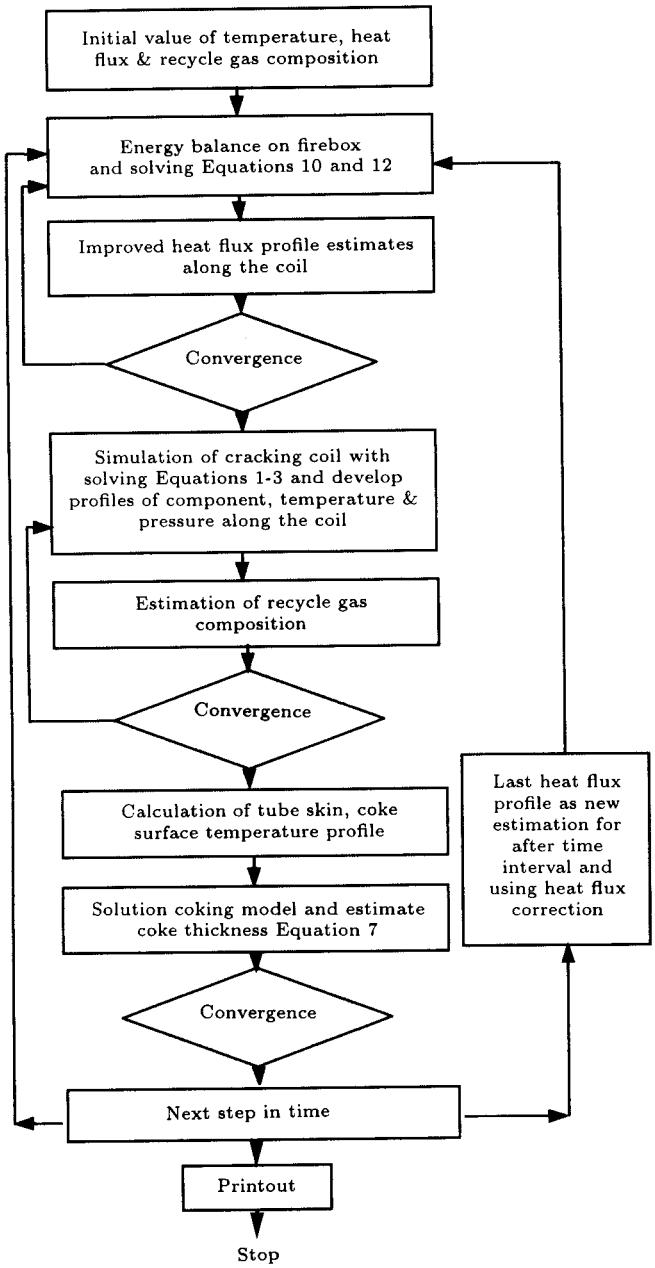

Figure 5. Simplified flow chart of calculation of cracking coils.

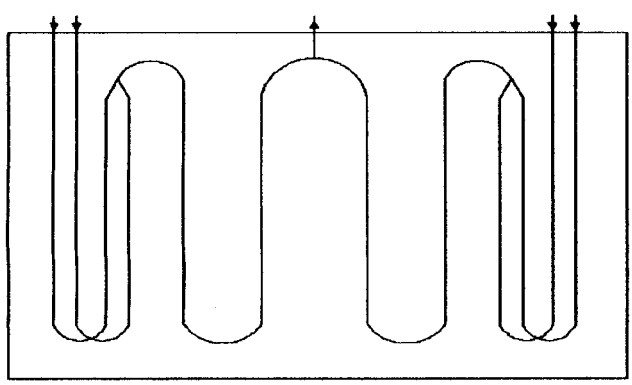

Figure 6. Configuration of industrial cracking coils.

Table 3. Basic information of furnace.

Furnace Characteristics	
Height (m)	11.473
Length (m)	10.488
Depth (m)	2.1
No. of burners	108
Reactor Configuration	
Total length (m)	45
For length (m):	22.5
I.D. (mm)	85
O.D. (mm)	92
For length (m):	45
I.D. (mm)	121
O.D. (mm)	130
Material Properties	
Tube thermal conductivity(W/m. K)	-1.257 + 0.0432 T
Coke thermal conductivity(W/m. K)	6.46
Coke specific gravity (kg/m^3)	1680

Table 4. Feed and operating conditions.

Operating Conditions			
HC flow rate (kg/hr/furnace)			11600
Recycle gas flow rate (kg/hr/furnace)			802.83
Steam dilution (kg steam/kg HC)			0.7
Coil inlet temp. (°C)			603
Coil inlet pressure at start of run (bar)			2.15
Feed Composition (wt%)			
C_4	4.65	2,2,3,TM butane	10.6
i-C_5	16.48	Aromatics	2.94
n-C_5	22.52	c-C_6	7.13
c-C_5	7.39	n-C_7	1.69
2 M pentane	13.65	C_8 & C_9	0.93
n-C_6	12.02		

Table 5. Furnace firing details.

Calculation basis (°C)	25
Fuel molecular weight (kg/kmole)	14.14
Lower heating value (kcal/kmole)	173550
Lower heating value (kcal/kg)	12277
Fuel gas temperature (°C)	10
Air temperature (°C)	10
Excess air	15%
Firebox pressure (kg/Cm^2)	0.85
O_2.stoic	1.7936
O_2.act	2.0626
Air (kmole air/fuel)	9.9728
Fired heat (kcal/hr)	23846000
Heat flux of one burner (kcal/hr)	220800
Fuel flow to the side burners (kmole/hr)	137
Air flow to the side burners (kmole/hr)	1370

Table 6. Flue gas properties [17]

Molecular weight (kg flue/kmol flue)	27.66
Flue (mole.flue/mole.fuel)	10.902
TOT (Flue gas flow rate kg/hr)	41435
Flue gas specific heat (kcal/kg. °C)	0.33527
Flue gas enthalpy (kcal/kg)	435.8
Enthalpy in flue gas leaving (kcal/hr)	1805700
Flue gas viscosity (Cpoise)	0.05
Composition (%wt):	
CO_2	12.72
H_2O	12.96
O_2	2.88
N_2	71.44

Table 7. Cracking furnace dimensions.

Floor to roof (m)	11.473
End wall to end wall (m)	10.48
Side wall to center line of tubes (m)	1.05
Nr of end wall zones	22
Nr of roof zones	4
Nr of bottom zones	4
Nr of cold plane zones	44
Nr of gas cube zones	44
Average beam length (m)	1.54
Zone dimentions (m)	1.05
Convection coefficient (kcal/hr.m^2. °C)	29.214
Gas emissivity (at 1220.°C)	0.224
Gas absorptivity (at 1064.9°C)	0.2283
Weight factor at Tg (AG)	0.3348
Weight factor at Tr (AR)	0.3622

be simulated. The furnace is heated by 108 burners positioned in eight rows at both front and rear walls and the furnace is divided into zones by means of four equidistant horizontal planes. For lack of symmetry, all eight circumferential zones per axial division, skin temperature and recycled gas components, are the main parameters, which can be altered in the model. The results of the model include; coil outlet conditions, coke thickness, the composition profiles of species along the reactor and thermal conditions of the firebox.

RESULTS AND DISCUSSION

The results of the simulation program are illustrated in Figures 7 to 12 and Tables 8 to 10. Table 8 shows a comparison between the simulation results and plant output data at different on stream times of the furnace and good agreement is observed between these results, especially in main product yields. Figure 7 shows the ethylene yield over the run length of the reactor. The feed flow rates were also kept constant over the run length. The growth of the coke layer and the amount

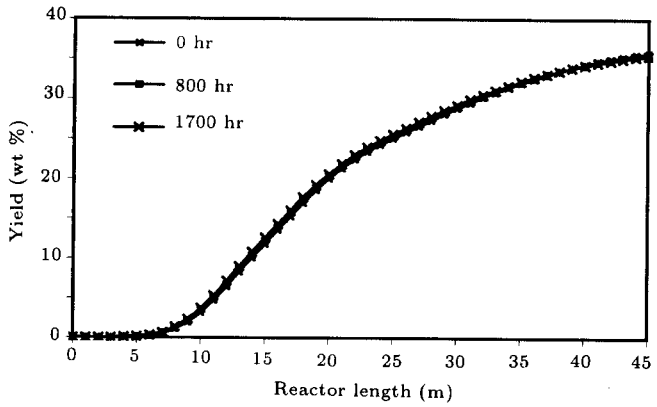

Figure 7. Variation of ethylene yield along the coil at different run length.

of heat transferred to the reacting process gas and pressure level are factors which affect the ethylene yield and selectivity. As shown in this figure, the ethylene yield is approximately constant over the run time of the reactor.

Figure 8 also shows that coking rate is increased in the first part of the reactor. The coke formation takes place at the temperature of the gas/coke interface. The coking rates are high in the second part of the reactor so that the concentration of coke precursors in the high temperature zone of the reactor is high. As a consequence, the coke layer grows fast in that area, creating an additional resistance to heat transfer and causing a decrease in the cross-sectional area of the tube. Increasing the heat fluxes also increases the gas/ coke interface temperatures and the coking rates, which means that the coke layer tends to become more uniform along the tube with time.

Figure 9 shows the simulated thickness of the coke layer as a function of run length. The coke deposition reaches its maximum thickness in the last pass at a length of 42 m, corresponding to a reduction in diameter of about 14%.

Figure 10 shows evolution of the heat flux profiles as a function of time, whereas, in the single tube

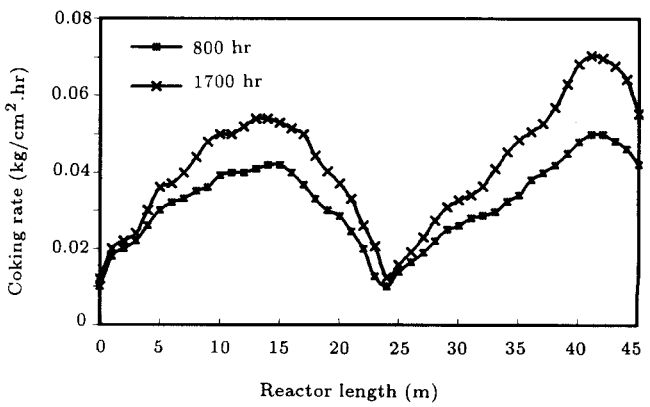

Figure 8. Variation of coking rate along the coil at different run length.

Table 8. Comparison of product yields of cracked gas at different run times (%wt).

	SOR(0 hr)		MOR (800 hr)		EOR (1700 hr)	
Component	**Simulation**	**Plant Data**	**Simulation**	**Plant Data**	**Simulation**	**Plant Data**
H_2	1.19	0.86	1.15	0.81	1.12	0.75
CH_4	17.72	17.1	17.38	6.79	17.43	16.64
C_2H_2	0.9	1.08	0.86	1.05	0.8	1.03
C_2H_4	35.7	35.4	35.07	35.00	34.22	34.08
C_2H_6	5.72	6.04	6.08	6.21	6.42	6.46
C_3H_6	12.14	12.75	12.75	13.12	13.04	13.35
C_3H_8	0.46	0.43	0.53	0.45	0.57	0.45
C_4H_6	3.98	4.5	4.22	4.78	4.14	4.92
C_4H_8	1.47	2.54	2.85	2.69	3.01	2.85
C_4H_{10}	0 0.25	0.35	0.29	0.4	0.31	0.47
Aromatic	9.67	10.02	10.69	10.25	10.66	9.68

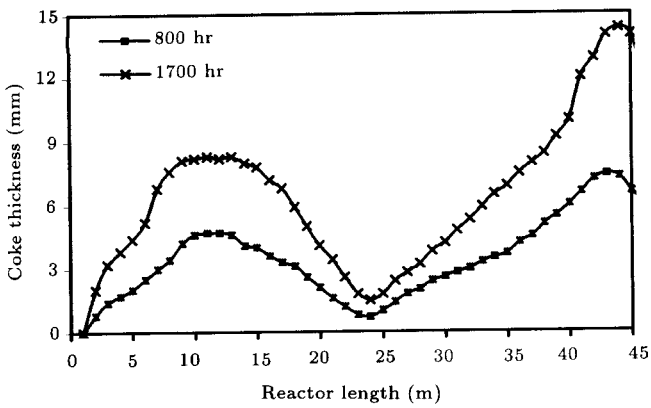

Figure 9. Variation of coke thickness at different run length.

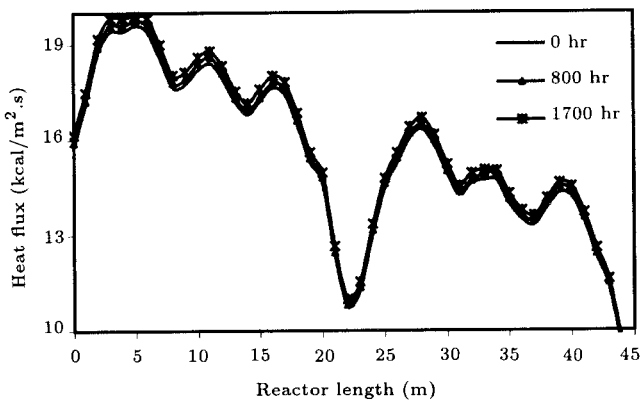

Figure 10. Variation of heat flux profile in the length of reactor at different run time.

section, the heat flux decreases with time. The high heat fluxes in the first part of the reactor result from the requirement of achieving a higher conversion, so as to keep the ethylene yield constant, in spite of the increase in pressure. It compensates for the decrease of the heat fluxes in the second part of the reactor caused by the coke formation. The coke layer reaches its maximum thickness in the second part of the coil.

The resistance against heat transfer caused by the coke layer makes the external tube skin temperature rise, especially in the second section of the reactor. Figure 11 shows the evolution of the coke layer with time, which is reflected in the external wall temperatures. In the first section of the reactor, the temperature profile also shows a significant increase, however, this is mainly due to the higher heat flux and peaks in the external tube skin temperature profile corresponding with the bottom of the furnace. Maximum value is reached at the end of the second part. The run-time of the cracking furnace is limited by the external tube skin temperature. In the present case, the maximum allowable temperature at the second section of the coil is 1050°C, where run length is predicted to be 70 days and plant data to be 75 days.

Tables 9 and 10 show a comparison between the program and design data of the refractory temperature and flue gas temperature variations at different level positions, in four heated zones of the furnace and at the start of the running of the furnace, respectively.

Figure 12 illustrates the circumferential temperature variations at different radial positions of the tube.

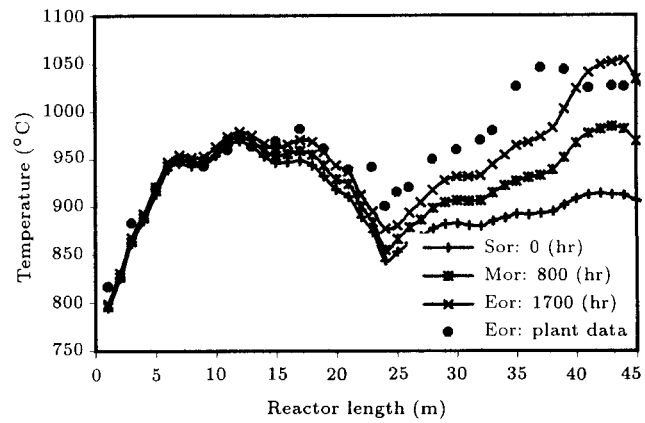

Figure 11. Profile of tube skin temperature in the length of reactor .

Table 9. Refractory temperature profile (°C).

	Zone 1		Zone 2		Zone 3		Zone 4	
Height(m)	Simulation	Spyro	Simulation	Spyro	Simulation	Spyro	Simulation	Spyro
10.95	991.8	989	1007.2	999	1027.1	1017	1048.5	1059
9.91	991.0	-	1007.0	-	1027.1	-	1048.5	-
8.87	1033.2	1044	1047.0	1038	1067.0	1054	1091.6	1098
7.83	1045.2	1032	1057.3	1048	1076.2	1063	1117.5	1106
6.79	1068.4	1068	1079.2	1070	1097.0	1084	1129.9	1125
5.75	1083.6	1084	1092.7	1085	1109.9	1097	1125.9	1137
4.71	1083.5	1085	1090.8	1084	1107.1	1095	1111.0	1133
3.67	1072.9	1076	1078.8	1075	1094.3	1084	1125.8	1120
2.63	1059.6	1064	1064.3	1063	1078.6	1071	1092.6	1103
1.59	1075.7	1081	1078.3	1079	1090.1	1085	1103.4	1112
0.55	1102.0	1106	1102.1	1104	1109.5	1108	1121.2	1130

Table 10. Flue gas temperature profile in firebox (°C).

	Zone 1		Zone 2		Zone 3		Zone 4	
Height(m)	Simulation	Plant Data	Simulation	Plant Data	Simulation	Plant Data	Simulation	Plant Data
10.95	1099.1	1097.5	1116.8	1116.4	1137.2	1135.8	1160.4	1159.4
9.91	1134.4	1134.2	1150.6	1151.5	1172.5	1172.5	1195.8	1195.5
8.87	1183.8	1185.9	1197.6	1200.9	1218.5	1220.6	1240.2	1242.1
7.83	1201.5	1202.2	1213.9	1216.0	1234.1	1234.8	1254.5	1255.3
6.79	1232.1	1228.9	1242.7	1241.1	1262.1	1259.2	1281.1	1278.6
5.75	1249.5	1252.6	1258.4	1263.4	1277.2	1280.6	1295.5	1298.8
4.71	1245.7	1249.7	1252.9	1259.6	1271.5	1276.1	1287.3	1293.3
3.67	1227.8	1334.4	1233.8	1242.7	1251.8	1258.7	1266.4	1274.6
2.63	1208.9	1190.7	1214.0	1210.7	1231.1	1226.2	1244.2	1240.7
1.59	1236.7	1212.6	1239.4	1230.4	1254.4	1234.6	1266.4	1257.8
0.55	1267.4	1255.0	1267.2	1268.8	1275.7	1276.6	1286.1	1290.1

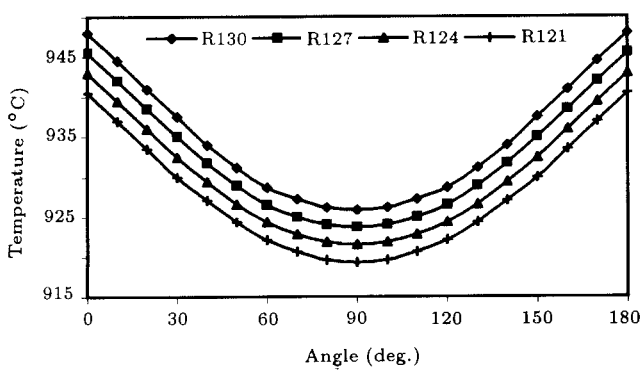

Figure 12. Circumferential tube temperature results on the reactor wall.

They clearly show that the maximum temperatures are always found at the zones which are facing the front walls (0 and 180 degrees) and which receive the maximum radiation from the furnace wall and the burners. The minimum temperatures occur at the zones on both sides of the tubes (90 and 270 degrees), due to the shadow effect of the neighboring tubes. Cracking furnaces are controlled on the basis of the process gas exit temperature and/or compositions. Thermocouples inserted at intermediate locations of the coil do not last very long, since the cracking temperature is too high. Therefore, the external tube skin temperature is measured, periodically, by the radiation pyrometers, through peepholes in the furnace walls.

The simulated results show that the observed temperatures depend upon the location of the peepholes, with respect to the tubes. The results of the model have been compared with the design data obtained from the plant. Unfortunately, except for the tube skin temperatures, which are measured by the pyrometer, other thermal characteristics of the furnace, such as gas and refractory temperatures and heat flux measurement, are impossible to obtain or inaccurate. The comparison with plant data is made for only the tube skin temperature and other parameters are based on the design data obtained from the simulation network package of SPYRO, developed by the Pyrotech petrochemical company [18]. Non uniformity of temperature along the perimeter of the vertical coils is shown in Figure 12 and is considered

to be significant. Even with a coil, the difference in temperature between maxima and minima can be in the order of 30°C. However, these differences cannot always be detected, since temperature measurement relies upon the use of an infrared pyrometer, using peepholes in the walls of the furnace, so that only certain view angles are possible. The model and the simulation software presented here are used as a guide for plant operation in the Arak petrochemical complex, in order to control the furnace parameters.

CONCLUSION

A complete reaction network for the pyrolysis of naphtha is used for the simulation of naphtha pyrolysis and the calculated results show good agreement with the experimental data. Plant information was also combined to obtain a mechanistic insight into coke formation in thermal cracking. This coking model was combined with a rigorous kinetic model for the cracking and a reactor and furnace model were used to simulate the run length of a furnace for the thermal cracking of naphtha. Detailed and accurate information can be obtained from this simulation. The growth of a coke layer is accurately simulated, together with the evolution of the external tube skin temperatures. The simulated and plant observation run lengths are in satisfactory agreement. Simulations of this kind can be used to optimize furnace operation for various feedstock and operating conditions and as a guide for the adaptation of the operating variables, aimed at prolonging the run length of the cracking furnace.

ACKNOWLEDGMENT

The authors acknowledge the cooperation of the Olefin plant of the Arak Petrochemical Company of Iran in support of the process data for this work.

NOMENCLATURE

A_i	area of a zone (m^2)
C	accumulation of coke (m)
C_i	concentration of coke precursors (mole/m^3)
C_p	heat capacity (J/mole.°K)
d_t	tube diameter (m)
E_i	black body emissive power (W/m^2)
E_o	activation energy (J/mole)
F	molar flow rate (mole/hr)
Fr	friction factor
G	total mass flux of the process gas ($kg/m^2.s$)
h_p	process gas convection coefficient ($W/m^2.°K$)
$-\Delta H$	heat of reaction (J/mole)
k	thermal conductivity of tube (W/m.°K)
k_i	pre-exponential factor for coke formation (kg coke/(m^2)(hr)(kmol/m^3)^n)
k_o	rate constant of coking reactions (kg coke/(m^2)(hr)(kmol/m^3)^n)
M_m	average molecular weight (kg/mole)
n	reaction order for coking
P_t	total pressure (Kpa)
Q	heat flux (W/m^2)
R	gas constant (J/mole°. K)
R_b	radius of the tube bend (m)
Re	Reynolds number
r	tube radius (m)
r_c	coking reaction rate ($kg/m^3.s$)
r_{ri}	reaction rate of species i in pyrolysis process ($mole/m^3.s$)
t_c	coke thickness(m)
t	time (hr)
s_{ij}	stochiometery factor
T	temperature (°K)
Z_iZ_j	total exchange area from zone i to j (m^2)
Z	axial reactor coordinate (m)

Greek Letters

α	coking factor
Λ	angle of bend 0
ζ	parameter of tube bend
ρ_c	coke density(kg/m^3)
η	unit conversion factor
θ	tube perimeter angle

REFERENCES

1. *Simulation Software for the Naphtha Cracking Furnaces*, Tarbiat Modarres University, Chemical Engineering Department, Tehran, Iran (1999).
2. Towfighi, J. and Nazari, H. "Simulation of light hydrocarbons pyrolysis using radical mechanism", *APCCHE/CHEMECA*, **93**, Melbourne, Australia (1993).
3. Towfighi, J. and Karimzadeh, R. "Development of a mechanistic model for pyrolysis of naphtha", *APCCHE/CHEMECA*, **93**, Melbourne, Australia (1993).

4. Towfighi, J. and Karimzadeh, R. "Modelling and simulation of thermal cracking of heavy hydrocarbons through radical mechanisms", *3rd National Congress of Chem. Eng.*, Tehran, Iran (1998).

5. Heyndericks, G.J. and Froment, G.F. "Simulation and comparison of the run length of an ethane cracking furnace with reactor tubes of ...", *Ind. Eng. Chem. Res.*, **37**, p 914 (1998).

6. Lichtenstein, I. "Design cracking furnace", *Chem. Eng. Prog.*, **60**(12) (1964).

7. Albright, L.F and Marek, J.C. "Coke formation during pyrolysis", *Ind. Eng. Chem. Res.*, **27**, p 743 (1988).

8. Kopinke, F.D., Zimmermann, G. and Nowak, S. "On the mechanism of coke formation in steam cracking conclusions from results obtained by tracer experiments", Carbon, **56**(2), pp 117-124 (1988).

9. Kopinke, F.D., Zimmermann, G., Reyners, G. and Froment, G.F. "Relative rates of coke formation from hydrocarbons in steam cracking of naphtha. 2. Paraffins, naphthenes, ...", *Ind. Eng. Chem. Res.*, **32**(56) (1993).

10. Kopinke, F.D., Zimmermann, G., Reyners, G. and Froment, G.F. "Relative rates of coke formation from hydrocarbons in steam cracking of naphtha. 3.Aromatics", *Ind. Eng. Chem. Res.*, **32**(2620) (1993).

11. Towfighi, J., Niaei, A. and Hosseini, S. "Development of a kinetic model of coke formation in pyrolysis of naphtha", *Iranian Journal of Science and Technology* (in press) (2001).

12. Hottel, H.C. and Sarofim, A.F. "Radiative heat transfer", McGraw Hill, New York, USA (1967).

13. Paramenswaran, A.K. and Sharma, V.K. "Modelling of naphtha pyrolysis in the swagged coils", *Can. J. Chem. Eng.*, **66**(957) (1988).

14. Sadrameli, M. "Heat transfer calculation in the firebox of the ethylene plant furnaces", *Int. J. of Eng.*, **10**(4), p 219 (1997).

15. Rao, M.V.R., Pleheirs, P.M. and Froment, G.F. "The coupled simulation of heat transfer and reaction in a pyrolysis furnace", *Chem. Eng. Sci.*, **43**, p 1223 (1988).

16. Heynderickx, G.J. and Cornelis, G.G. "Circumferential tube skin temperature profiles in thermal cracking coils", *AIChE J.*, **38**(12), p 1905 (1992).

17. Reid, R.C., Prausnitz, J.M. and Poling, B.E., *The Properties of Gases and Liquids*, McGraw Hill Book Co. (1988).

18. Dente, M., Ranzi, E. and Goossens, A.G. "Detailed prediction of olefin yields from hydrocarbon pyrolysis through a fundamental simulation model (SPYRO)", *Comput. Chem. Eng.*, **3**(61) (1979).